



## SHORT COMMUNICATION

# miR-133b Regulation of Connective Tissue Growth Factor

## *A Novel Mechanism in Liver Pathology*

Altin Gjymishka,\* Liya Pi,\* Seh-Hoon Oh,\* Marda Jorgensen,\* Chen Liu,<sup>†</sup> Yianni Protopapadakis,\* Ashnee Patel,\* and Bryon E. Petersen\*

From the Departments of Pediatrics\* and Pathology, Immunology, and Laboratory Medicine,<sup>†</sup> University of Florida, Gainesville, Florida



Accepted for publication  
December 28, 2015.

Address correspondence to  
Bryon E. Petersen, Ph.D.,  
Department of Pediatrics,  
University of Florida College of  
Medicine, PO Box 100269,  
Gainesville, FL 32610-  
0275. E-mail: [bryonpetersen@  
peds.ufl.edu](mailto:bryonpetersen@peds.ufl.edu).

miRNAs are involved in liver regeneration, and their expression is dysregulated in hepatocellular carcinoma (HCC). Connective tissue growth factor (CTGF), a direct target of miR-133b, is crucial in the ductular reaction (DR)/oval cell (OC) response for generating new hepatocyte lineages during liver injury in the context of hepatotoxin-inhibited hepatocyte proliferation. Herein, we investigate whether miR-133b regulation of CTGF influences HCC cell proliferation and migration, and DR/OC response. We analyzed miR-133b expression and found it to be down-regulated in HCC patient samples and induced in the rat DR/OC activation model of 2-acetylaminofluorene with partial hepatectomy. Furthermore, overexpression of miR-133b via adenoviral system *in vitro* led to decreased CTGF expression and reduced proliferation and Transwell migration of both HepG2 HCC cells and WBF-344 rat OCs. *In vivo*, overexpression of miR-133b in DR/OC activation models of 2-acetylaminofluorene with partial hepatectomy in rats, and 3,5-diethoxycarbonyl-1,4-dihydrocollidine in mice, led to down-regulation of CTGF expression and OC proliferation. Collectively, these results show that miR-133b regulation of CTGF is a novel mechanism critical for the proliferation and migration of HCC cells and OC response. (*Am J Pathol* 2016, 186: 1092–1102; <http://dx.doi.org/10.1016/j.ajpath.2015.12.022>)

Liver has the unique ability to self-regenerate from both mature hepatocytes and facultative stem cells, usually referred to as hepatic progenitor cells (HPCs) in humans and mice, or oval cells (OCs) in rats.<sup>1</sup> HPCs mediate liver regeneration by producing new hepatocyte lineages during liver injury in the context of inhibition of hepatocyte proliferation by hepatotoxins.<sup>2</sup> Experimental models of OC activation in rats use two-thirds partial hepatectomy (PHx) in combination with inhibitors of hepatocyte proliferation, such as 2-acetylaminofluorene (2-AAF) or the pyrrolizidine alkaloid retrorsine.<sup>3–5</sup> In the context of the 2-AAF/PHx model, OCs that appear as small, poorly differentiated, and rapidly proliferating cells arise in periportal areas [ie, OC response or ductular reaction (DR)] and are able to differentiate into hepatocytes and bile ductular epithelial cells.<sup>2,6</sup> Alternatively, 3,5-diethoxycarbonyl-1,4-dihydrocollidine (DDC) feeding of mice represents a xenobiotic model of cholestatic liver injury that induces DRs and biliary

fibrosis.<sup>7,8</sup> There is a dual function of HPCs/DRs in both liver regeneration and liver fibrosis. DRs are associated with the liver regenerative response but, in the case of persistent stimuli (ie, chronic injury) DRs are also involved in liver fibrogenesis.<sup>1</sup> We have found that connective tissue growth factor (CTGF), a secreted matricellular protein, is highly up-regulated in HPCs/OCs and cholangiocytes after liver damage.<sup>9</sup> CTGF protein, through its four conserved modules that interact with ECM proteins, growth factors, and receptors (ie, integrin  $\alpha v \beta 6$ ), plays pleiotropic roles on different cell types and tissues.<sup>10,11</sup> Both the OC activation and the fibrotic response in the liver are suppressed after

Supported by NIH grants DK058614 and DK065096 (B.E.P.) and American Cancer Society Chris DiMarco Institutional Research grant (L.P.).

A.G. and L.P. contributed equally to this work.

Disclosures: None declared.

down-regulation of CTGF in animal models.<sup>9,12</sup> Despite these important findings, signaling pathways and molecular mechanisms that control OC activation in liver regeneration remain largely unknown.

Mammalian miRNAs are short, approximately 22 nucleotides, highly conserved RNAs.<sup>13</sup> These endogenous non-coding RNAs bind to the 3' untranslated region (UTR) of their target genes and repress their translation.<sup>14</sup> There are two main circuits through which miRNAs regulate expression of their targets. miRNA and its target can either be coexpressed (positive correlation) in an incoherent circuit or have anti-correlation showing coherent regulation. miRNA/target coexpression and positive correlation, mainly present in mechanisms involved in homeostasis, have been demonstrated for miRNAs, such as miR-430 or miR-124, and denote fine tuning of the target mRNA expression.<sup>15–17</sup> Recent studies have demonstrated that miRNAs are important in OC activation and development of hepatocellular carcinoma (HCC).<sup>18,19</sup> HCC represents 90% of primary liver cancers, it has poor prognosis, and its incidence is increasing worldwide.<sup>20</sup> A study from Gailhouse et al<sup>21</sup> identified direct targeting of DNA methyltransferase 1 by the hepatospecific miR-148a (down-regulated in HCC patients, mouse, and human HCC cell lines) to be critical for hepatic differentiation. miRNA expression is dysregulated in various types of cancer, including HCC.<sup>19,22,23</sup>

The miR-133 family (miR-133a-1, miR-133a-2, and miR-133b) is among the most studied miRNAs.<sup>24</sup> These miRNAs are transcribed as bicistronic RNAs together with miR-1-2, miR-1-1, and miR-206, respectively. miR-133 family members are important in muscle (ie, myomiR) development, myocardial matrix remodeling, and apoptotic signaling.<sup>25,26</sup> miR-133a was shown to play an antifibrotic role in the liver, representing a target for diagnosis and treatment of liver fibrosis.<sup>27,28</sup> miR-133b has been shown to be decreased in colorectal cancer, esophageal squamous cell carcinoma, and lung and bladder cancer.<sup>25</sup> In human genome, miR-133b is part of the miR-206/miR-133b cluster located on chromosome 6p12.2. We have recently demonstrated that CTGF represents a direct target of miR-133b.<sup>29</sup> Although the role of CTGF in HCC is unclear, recent reports support a role in HCC growth and metastasis.<sup>30,31</sup> In the current study, we investigated miR-133b regulation of CTGF in HCC and OC activation models. We show that miR-133b is decreased in human HCC, it down-regulates CTGF expression, and it suppresses proliferation and migration of HepG2 cells, *in vitro*. Furthermore, miR-133b is significantly up-regulated in the liver of 2-AAF/PHx-treated rats and directly targets CTGF 3'UTR in WBF-344 OCs. Overexpression of this miRNA reduces OC activation induced by 2-AAF/PHx in rats or DDC in mice. Thus, miR-133b regulation of CTGF expression is a critical mechanism in the cell proliferation and migration of HCC cells and in the OC response. This mechanism could be manipulated therapeutically to either suppress liver tumor development or enhance liver regeneration.

## Materials and Methods

All animal experiments and patient sample analysis were performed in conformity with approved Institutional Animal Care and Use Committee and Institutional Review Board protocols at the University of Florida (Gainesville). Human liver samples were from patients of a tertiary care center, Shands Hospital at the University of Florida. The median age of this group was 54.5 years (range, 51 to 71 years), and they were all white (one female and seven males).

### Animal Models

#### Rat 2-AAF/PHx Model

In the rat OC activation protocol, continuous administration of 2-AAF was used to suppress proliferation of mature hepatocytes. A 2-AAF, time-release pellet was inserted into the peritoneal cavity of the rat. Hepatic injury was induced by a partial hepatectomy (66% resection of the liver), as described by Higgins and Anderson.<sup>32</sup> Intraportal injection of adenovirus,  $3 \times 10^{11}$  viral particles expressing green fluorescent protein (GFP) only (Ad-control) or GFP-miR-133b (Ad-miR-133b), was performed at the time of PHx.

#### Mouse DDC Model

Mice were given a 0.01% DDC diet, according to a previously published protocol.<sup>33</sup> Mice were injected on the tail vein with adenovirus ( $3 \times 10^{11}$  viral particles) expressing GFP only or GFP-miR-133b at day 1 after DDC treatment. On day 8, animals were sacrificed and liver tissues were analyzed.

### Cell Culture, Proliferation, and Transwell Migration Assays

HepG2 and HEK-293 cells were purchased from ATCC (Manassas, VA). WBF-344 cells were a gift from Dr. William B. Coleman (University of North Carolina at Chapel Hill). Huh-7 cells were obtained from Dr. Chen Liu's laboratory (University of Florida, Gainesville). All cell lines were cultured in high glucose (4.5 g/L) Dulbecco's modified Eagle's medium with 10% (v/v) fetal bovine serum, 1% penicillin, and streptomycin, in a humidified atmosphere of 5% CO<sub>2</sub>. Cells were cultured in T-75 flasks and passed when they reached 70% to 80% confluence. The maximum passage number was five. HepG2 and WBF-344 cells were used in the proliferation and Transwell migration assays.

#### Proliferation Assay

HepG2 or WBF-344 cells ( $1 \times 10^4$ ) in Dulbecco's modified Eagle's medium and 0.25% fetal bovine serum were inoculated into a 96-well plate and were serum starved for 24 hours. Then, 100 ng/mL recombinant CTGF and 1 ng/mL epidermal growth factor (Abcam, Cambridge, MA) were added in the cells. The total cell number in each well was assessed using CyQUANT NF cell proliferation assay kit (Invitrogen) at

**Table 1** Primer Sequences

Species	Gene	Primers
Human	<i>CTGF</i>	Forward: 5'-TGGAGATTTTGGGAGTACGG-3' Reverse: 5'-CAGGCTAGAGAAGCAGAGCC-3'
Human	<i>ACTB</i>	Forward: 5'-GATGAGATTGGCATGGCTTT-3' Reverse: 5'-GAGAAGTGGGGTGGCTT-3'
Human	<i>miR133b</i> (Adenovirus Insert)	Forward: 5'-GTCCCCCTCAACCAGCTACA-3' Reverse: 5'-GAGTGCAAAGGCACAGAACA-3'
Rat	<i>Ctgf</i>	Forward: 5'-GGATCCGACCATGCTCGCCTC-CGTCG-3' Reverse: 5'-TCCTCGAGCGCAGTTGGCTCGC-ATCA-3'
Rat	<i>Gapdh</i>	Forward: 5'-TGGAGAAACCTGCCAAGTAT-GA-3' Reverse: 5'-TGGTATTCGAGAGAAGGGAG-GG-3'
Mouse	<i>Ctgf</i>	Forward: 5'-AGTGGAGCGCCTGTTCTAAG-3' Reverse: 5'-GACAGGCTTGGCGATTTTAG-3'
Mouse	<i>18S</i>	Forward: 5'-TTGACGGAAGGGCACCACC-AG-3' Reverse: 5'-GCACCACCACCCACGGAAT-CG-3'

day 0 to 3 after plating. Fluorescence was measured using a microplate reader with excitation at 497 nm and emission detection at 520 nm. From each group, samples were used in triplicate.

Transwell Migration Assay

HepG2 or WBF-344 cells that were transduced with control or miR-133b viruses were trypsinized and resuspended in Dulbecco’s modified Eagle’s medium and 0.25% fetal bovine serum. A total of 2 × 10<sup>4</sup> cells were inoculated in the upper chamber of Transwells in 24-well companion plates (Corning Inc., Lowell, MA). The pore size was approximately 5.0 μm for HepG2 and 8.0 μm for WBF-344 cells. Cells were incubated in the presence or absence of 250 ng/mL recombinant human CTGF (Peprotech, Rocky Hill, NJ) in the lower chamber. Six hours later, the Transwell membrane was fixed with ice-cold methanol for 1 minute. Cell staining solution (Trevigen, Gaithersburg, MD) was applied to stain cells on the undersurface of the Transwells. Migrated cells were counted in 10 random fields at ×20 magnification. Data were obtained from samples in triplicate for each group.

Adenovirus Amplification and Purification

The GFP control and GFP-miR-133b premade adenoviruses were purchased from Vigene (Rockville, MD). Virus amplification was performed in HEK-293 cells that were cultured in 225-cm<sup>2</sup> flasks. A Virabind adenovirus purification kit (Cell Biolabs, Inc., San Diego, CA) was used for purification, according to the manufacturer’s instructions. Relative virus titer determination and infectivity were calculated on the basis of viral genome copy number determined by quantitative

PCR and green fluorescence from transduced HEK-293 cells, respectively.

Immunofluorescence, Immunohistochemistry, and Antibodies

Immunofluorescence and immunohistochemistry were performed in standard protocols with antibodies against GFP, CTGF, Ki-67, CK19, and A6.<sup>33</sup> Antibody against SOX9 (Millipore, Temecula, CA) was used to stain OCs in the 2-AAF/PHx model.

Western Blot Analysis

Whole cell extracts from rat livers were prepared for immunoblot analysis and were quantified by a Bio-Rad DC Protein assay; 30 μg of protein was separated on a Bolt 12% Bis Tris Plus pre-cast gel (Novex, Life Technologies/Thermo Fisher, Waltham, MA). Immunoblotting was performed using a primary antibody against CTGF purchased from Abcam in 5% blocking solution overnight at 4°C with mixing. To provide a demonstration of equal loading, membranes were reprobed with a 1:5000 dilution of an antibody specific for actin (Abcam).

Total RNA Isolation and RT-PCR

Total RNAs were extracted using the RNeasy Mini kit (Qiagen, Valencia, CA). Total RNA was incubated with RNase-free DNaseI (Qiagen) to remove any genomic DNA contamination. Template cDNA was obtained by reverse transcription of 100 ng of total RNA using reverse transcriptase Superscript III First-Strand Synthesis with 50 pmol random hexamer (Invitrogen). Semiquantitative RT-PCR analysis was performed to determine mRNA levels of rat *Ctgf* and *Gapdh*, mouse *Ctgf* and *18S*, and human CTGF and actin. Primer sequences are listed in Table 1.

TaqMan miRNA RT-PCR

After 2-AAF/PHx, rat liver tissues from normal and 2-AAF/PHx-treated animals were harvested, and miRNAs were isolated using a mirVANA miRNA isolation kit purchased from Life Technologies. Next, a TaqMan miRNA Reverse Transcription kit (Life Technologies) was used for reverse transcription reaction. TaqMan 2x Universal PCR Master-Mix II, No AmpErase UNG (Life Technologies) was used for real-time PCR. Both the miRNA reverse transcription and the real-time PCR were performed according to the manufacturer’s instructions. Small nucleolar RNA for rats, U6 snRNA for mice, and RNU6B RNA for human samples were used for miRNA expression normalization.

ISH and RT-PCR ISH

*In situ* hybridization (ISH) was performed to detect *Ctgf* mRNA expression, according to a previously reported

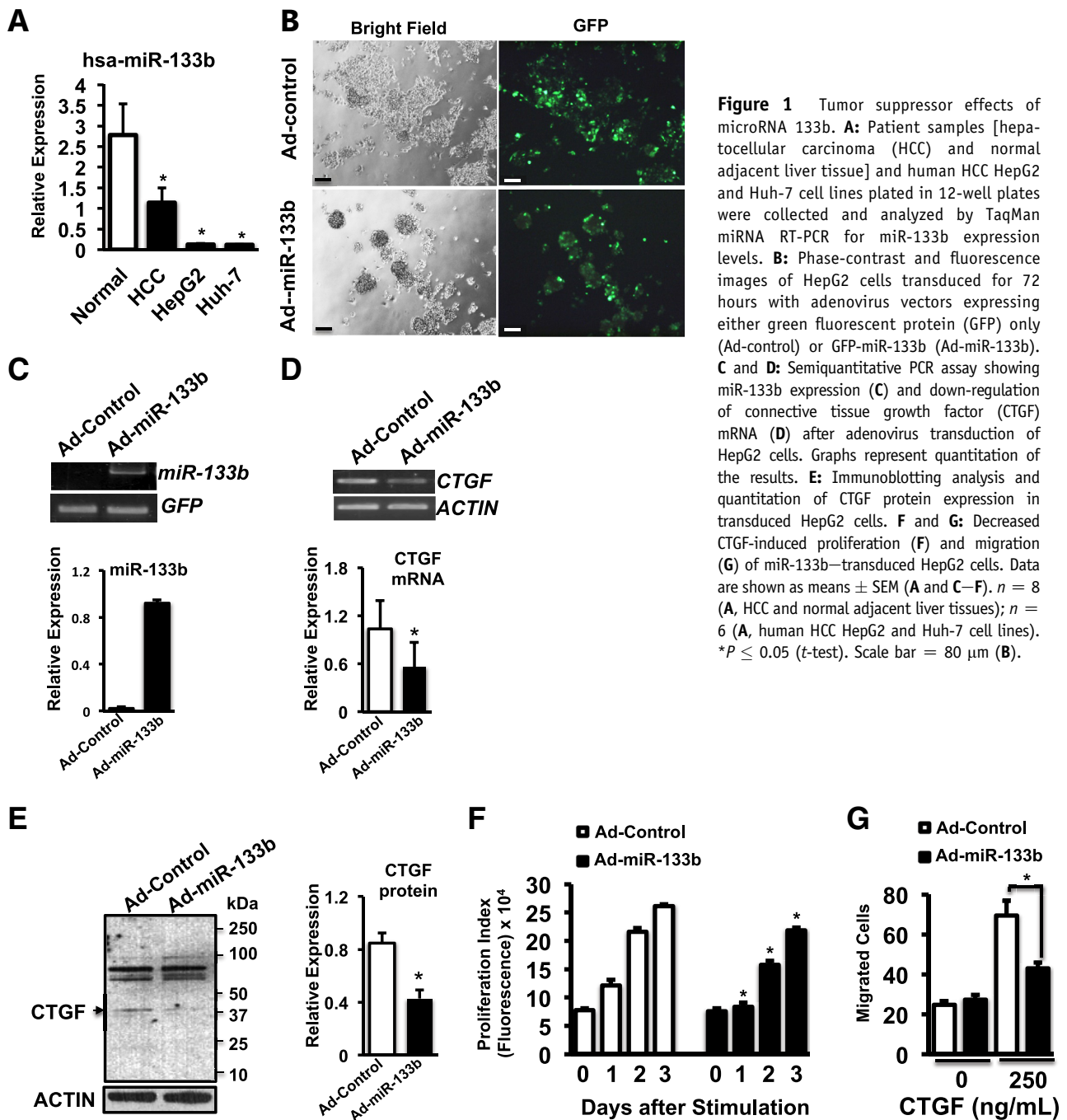


**Figure 1** Tumor suppressor effects of microRNA 133b. **A:** Patient samples [hepatocellular carcinoma (HCC) and normal adjacent liver tissue] and human HCC HepG2 and Huh-7 cell lines plated in 12-well plates were collected and analyzed by TaqMan miRNA RT-PCR for miR-133b expression levels. **B:** Phase-contrast and fluorescence images of HepG2 cells transduced for 72 hours with adenovirus vectors expressing either green fluorescent protein (GFP) only (Ad-control) or GFP-miR-133b (Ad-miR-133b). **C** and **D:** Semiquantitative PCR assay showing miR-133b expression (**C**) and down-regulation of connective tissue growth factor (CTGF) mRNA (**D**) after adenovirus transduction of HepG2 cells. Graphs represent quantitation of the results. **E:** Immunoblotting analysis and quantitation of CTGF protein expression in transduced HepG2 cells. **F** and **G:** Decreased CTGF-induced proliferation (**F**) and migration (**G**) of miR-133b-transduced HepG2 cells. Data are shown as means  $\pm$  SEM (**A** and **C–F**).  $n = 8$  (**A**, HCC and normal adjacent liver tissues);  $n = 6$  (**A**, human HCC HepG2 and Huh-7 cell lines).  $*P \leq 0.05$  ( $t$ -test). Scale bar = 80  $\mu$ m (**B**).

protocol.<sup>12</sup> Furthermore, to increase our ability to detect and localize miRNAs that are expressed at relatively low levels, we performed RT-PCR ISH. The paraffin-embedded sections were deparaffinized and rehydrated. Before antigen retrieval in 0.1 mol/L sodium citrate (pH 6.0), reverse transcription, followed by PCR incorporating 1 mmol/L DIG-11-dUTP (Roche, Indianapolis, IN), was performed on the sections. Positive signals were detected by alkaline phosphatase-conjugated antidigoxigenin and then enzymatic development using 4-nitro-blue tetrazolium and 5-brom-4-chloro-3'-indolylphosphate substrate (Roche) forming dark blue 4-nitro-blue tetrazolium-formazan precipitate.

Nuclear fast red (Vector Laboratories, Burlingame, CA) was used as a counterstain. Light microscopy was used to visualize the RT-PCR ISH signal.

#### Luciferase Activity Assay

WBF-344 cells, seeded at a cell density of  $35 \times 10^3$  in 48-well plates, were first transduced with adenovirus. After 24 hours, cells were transfected with 1  $\mu$ g per CTGF 3'UTR containing plasmid (GeneCopoeia, Inc., Rockville, MD). Purefection 2000 (System Biosciences, Mountain View, CA) transfection agent and Dual Luciferase Reporter Assay System (Promega,



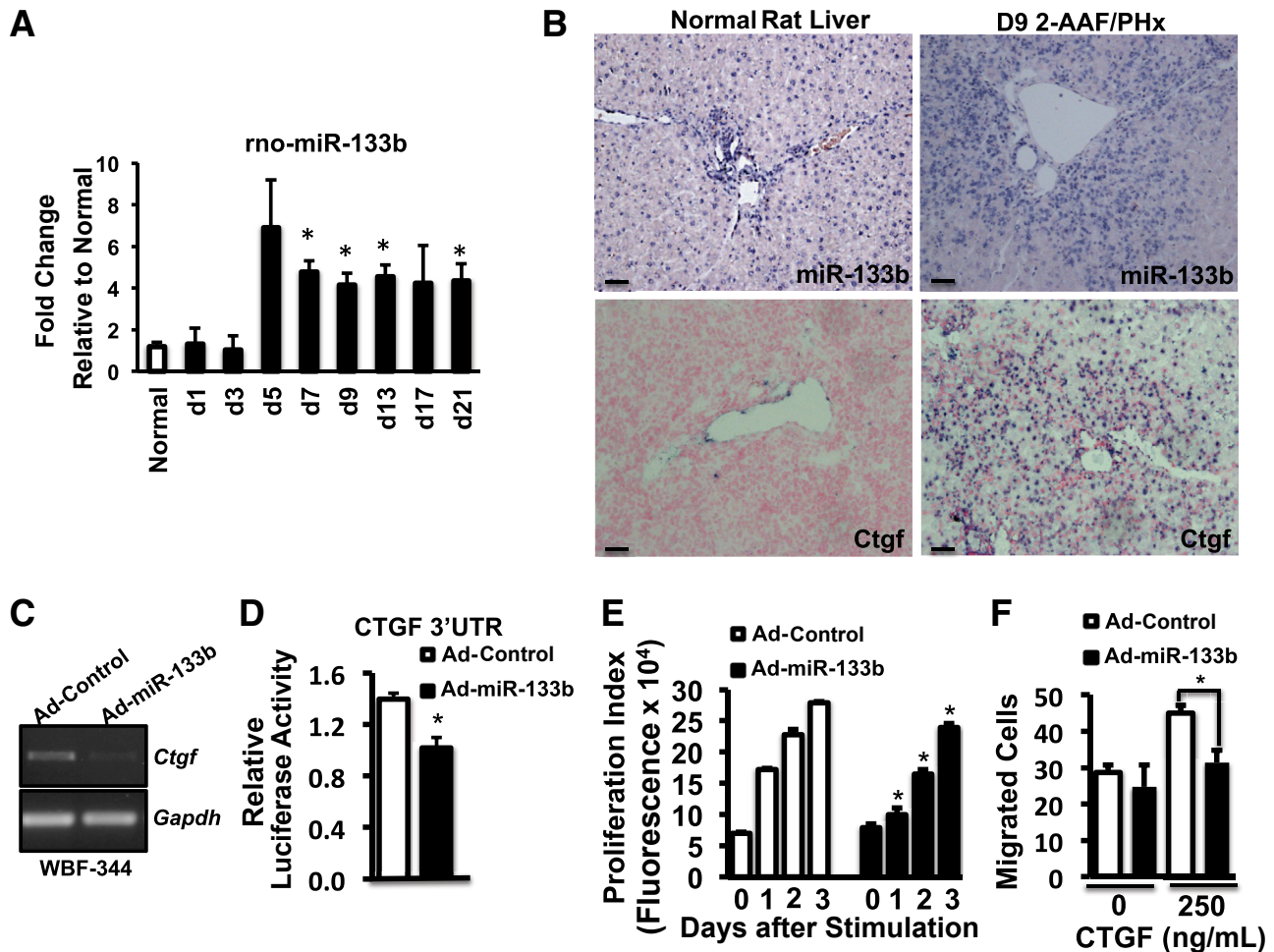


**Figure 2** Induction of miR-133b expression after 2-acetylaminofluorene (2-AAF)/partial hepatectomy (PHx) and *in vitro* effects of miR-133b overexpression in WBF-344 rat oval cells. **A:** Time course of the miR-133b expression in the rat liver tissues collected from normal and 2-AAF/PHx-treated animals from day (d) 1 to day 21. **B:** Induction of miR-133b expression and connective tissue growth factor (CTGF) mRNA by 2-AAF/PHx was assayed by RT-PCR *in situ* hybridization (ISH) and Ctgef ISH, respectively. **C:** Endogenous Ctgef and Gapdh mRNA levels in transduced WBF-344 for 72 hours were assayed by semi-quantitative PCR. **D:** Transduced WBF-344 cells were transfected with CTGF 3' untranslated region containing plasmid, and luciferase reporter assay was performed 48 hours after transfection. **E and F:** Reduction of the CTGF-induced proliferation (**E**) and migration of WBF-344 cells overexpressing miR-133b (**F**). Data are shown as the means  $\pm$  SEM (**A and D–F**).  $n = 6$  (**D**);  $n = 3$  (**A**, rats per time point, **E**, and **F**). \* $P \leq 0.05$  (*t*-test). Scale bar = 50  $\mu$ m (**B**).

Madison, WI) were used according to the manufacturer's instructions. A multiwell plate-reading luminometer was used for the measurements. Firefly luciferase activity was normalized to renilla.

### Statistical Analysis

Microsoft Excel software version 15.18 (Microsoft Corp., Redmond, WA) and *t*-test were used for statistical analysis.  $P \leq 0.05$  was considered statistically significant. Data are shown as means  $\pm$  SEM.

## Results

### miR-133b Functions as a Tumor Suppressor in the Liver

miR-133b has been shown to be a tumor suppressor in tongue squamous cell carcinoma, esophageal squamous

cell carcinoma, and colorectal cancer.<sup>34–36</sup> Whether miR-133b expression is altered in HCC is currently unknown. We analyzed patient HCC samples, and the data showed that miR-133b expression was decreased by 2.4-fold ( $2.78 \pm 0.76$  in normal versus  $1.14 \pm 0.35$  in HCC;  $P < 0.04$ ,  $n = 8$ ) relative to adjacent unaffected human liver tissue (Figure 1A). Similarly, we analyzed basal miR-133b expression in two human HCC cell lines, and it was determined to be low in both HepG2 ( $0.12 \pm 0.03$ ;  $P < 0.04$ ) and Huh-7 ( $0.12 \pm 0.01$ ;  $P < 0.04$ ) cells relative to miR-133b expression of normal human liver tissue. Next, because of the altered miR-133b expression in various types of cancer and the observed decrease of miR-133b in human HCC samples, we decided to analyze *in vitro* the expression of a direct miR-133b target in human HCC HepG2 cells after overexpression of miR-133b via an adenovirus delivery system. CTGF represents a direct miR-133b target that is expressed in HepG2 cells. A high transduction efficiency (Figure 1B) and miR-133b expression

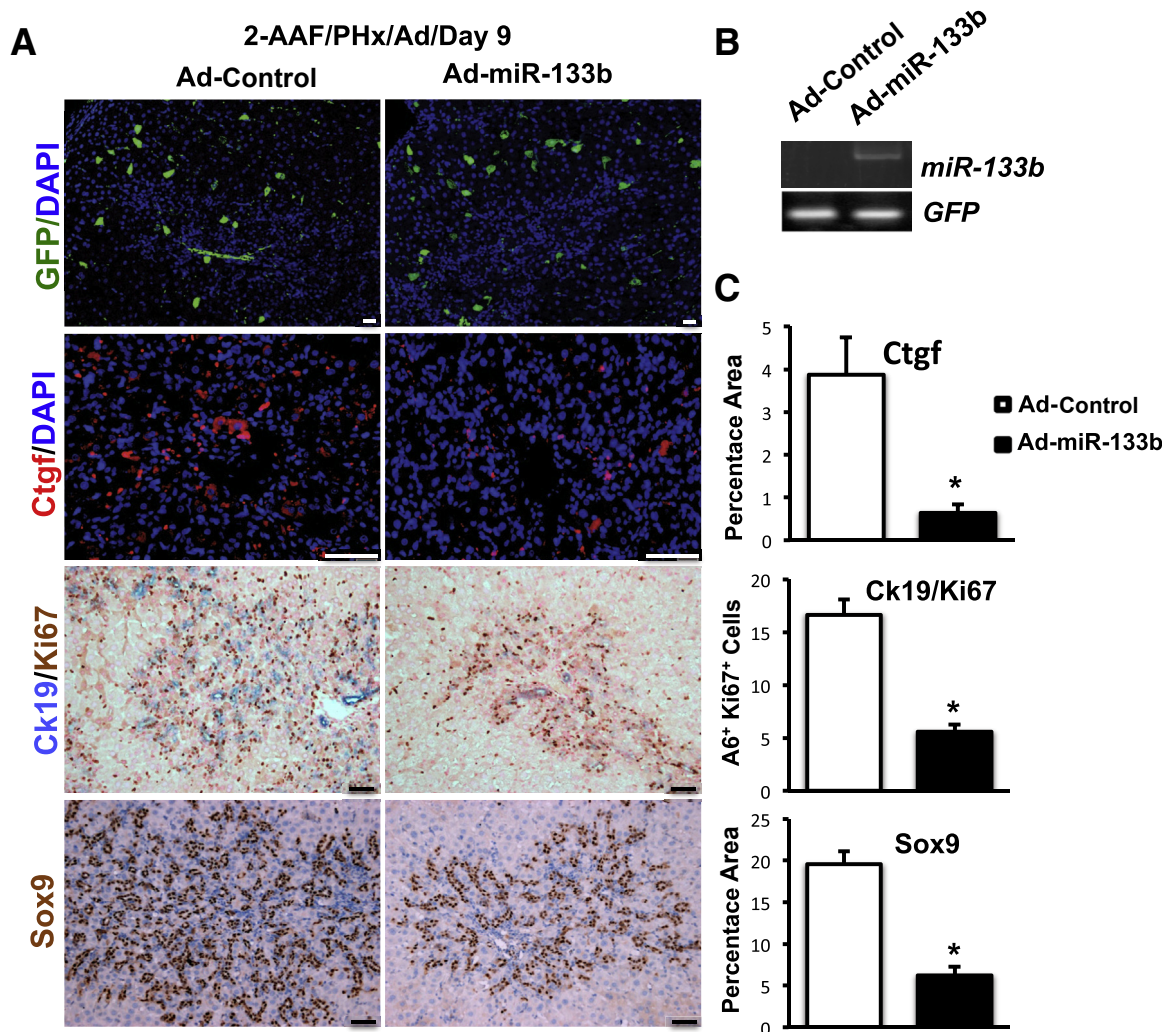


**Figure 3** Overexpression of miR-133b via adenoviral transduction system *in vivo* leads to down-regulation of connective tissue growth factor (CTGF) expression and oval cell response. Adenovirus vectors containing either green fluorescent protein (GFP)-control or GFP-miR-133b were delivered via intraportal injection at the time of 70% partial hepatectomy (PHx). Animals were sacrificed at day 9 after PHx. **A:** Paraformaldehyde-fixed and paraffin-embedded liver tissue sections were stained with immunofluorescence anti-GFP (green) antibody, anti-CTGF (red); and costained for Ck19 and Ki-67 or anti-Sox9. For the GFP and CTGF staining, slides were counterstained with DAPI (blue) for nuclear visualization. **B:** Semiquantitative PCR showing GFP and miR-133b transduction of rat livers. **C:** Graphs represent quantitation performed by ImageJ software version 1.48v (NIH, Bethesda, MD; <http://imagej.nih.gov/ij/>). Six to 12 images obtained from stained slides of three different rat livers were used for quantitation. Data are presented as means  $\pm$  SEM (**C**). \* $P < 0.05$  (*t*-test). Scale bar = 50  $\mu$ m (**A**). 2-AAF, 2-acetylaminofluorene.

(Figure 1C) were achieved in HepG2 cells at day 3, the time at which we analyzed CTGF expression. The semiquantitative PCR data showed a reduction in the mRNA expression level of CTGF in cells overexpressing miR-133b, relative to the levels observed in GFP-control transduced cells (Figure 1D). Furthermore, Western blot analysis of CTGF protein showed decreased levels in HepG2 cells overexpressing miR-133b relative to control cells (Figure 1E). In addition, miRNAs have been shown to play a tumor suppressor role in several cancer types, by affecting cancer cell proliferation and/or migration. To investigate if miR-133b has similar effects on HepG2 cells, we transduced cells with control or miR-133b-expressing adenoviral vectors and performed proliferation and migration assays. There was a significant decrease in the proliferation index of miR-133b-overexpressing HepG2 cells at day 1 ( $31.0\% \pm 6.0\%$ ;  $P < 0.01$ ), day 2 ( $27.0\% \pm 3.3\%$ ;

$P < 0.01$ ), and day 3 ( $16.3\% \pm 1.9\%$ ;  $P < 0.01$ ) after CTGF stimulation relative to control cells (Figure 1F). Next, HepG2 cells were seeded in Transwells and stimulated with 250 ng/mL recombinant CTGF or left unstimulated to study migration (Figure 1G). CTGF-induced migration of HepG2 cells with forced expression of miR-133b was significantly reduced ( $38.0\% \pm 1.9\%$ ;  $P < 0.03$ ) relative to control cells not overexpressing miR-133b (Figure 1G).

#### Induction of miR-133b during 2-AAF/PHx and *in Vitro* Effects of Ectopic miR-133b Expression on WB-F344 Rat OCs

miRNAs have been shown to be important in liver regeneration and stem cell development.<sup>18,37</sup> To explore if miR-133b expression is modulated during the OC activation



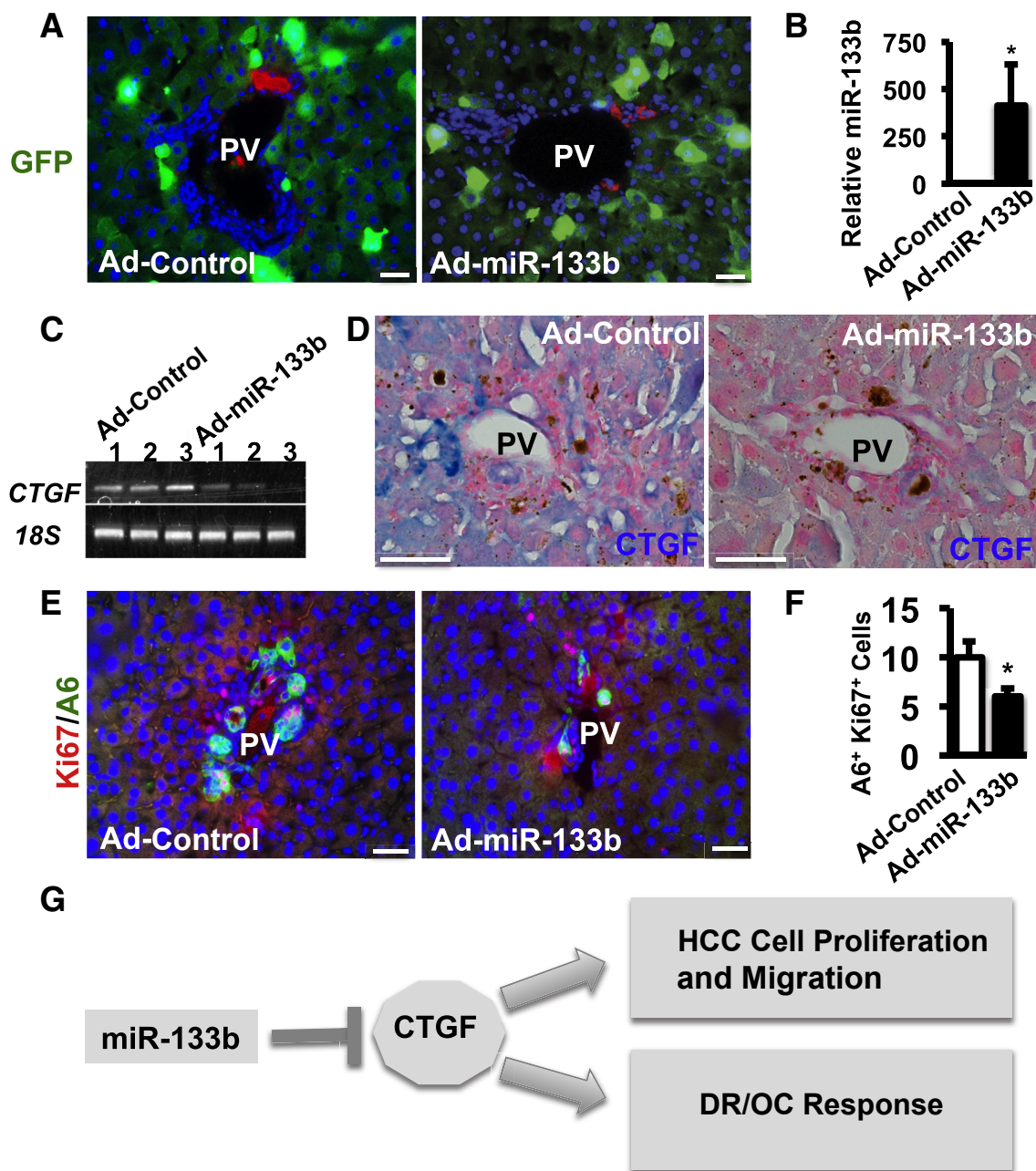


**Figure 4** *In vivo* delivery of miR-133b in 3,5-diethoxycarbonyl-1,4-dihydrocollidine (DDC)-treated mice reduces ductular reactions and oval cell proliferation. Mice that were given the DDC diet for 1 day were injected on the tail vein with adenovirus expressing green fluorescent protein (GFP) only (Ad-control) or GFP-miR-133b (Ad-miR-133b) and were fed a DDC diet for an additional 8 days. Animals were sacrificed, and liver tissues were analyzed. **A:** The immunofluorescence staining for GFP shows localization of transduced adenovirus in DDC-damaged livers. Red represents autofluorescence obtained from porphyrin plugs. **B:** TaqMan real-time PCR analysis detects high levels of miR-133b in infected livers. **C** and **D:** Lower levels of connective tissue growth factor (CTGF) mRNA and protein are detected by RT-PCR (**C**) and immunohistochemistry (**D**). Three different animals from each group were analyzed. **E:** Dual immunofluorescence staining for Ki-67 and A6 was performed to detect proliferating biliary epithelial cells. **F:** Biliary cells positive for both A6 and Ki-67 were counted from eight slides from three different animals on the basis of dual staining for Ki-67 and A6. Nuclei were counterstained with DAPI (blue; **A** and **E**) or nuclear fast red (**D**). **G:** Diagram illustrates how miR-133b down-regulation of CTGF expression leads to the decrease of hepatocellular carcinoma (HCC) cell proliferation and migration and to the reduction of ductular reactions (DRs)/oval cell (OC) response during liver injury (ie, 2-acetylaminofluorene/partial hepatectomy in rats or DDC in mice). Data are shown as means  $\pm$  SEM (**B** and **F**). \* $P \leq 0.05$  (*t*-test). Scale bar = 75  $\mu$ m (**A**, **D**, and **E**). PV, portal vein.

model, we analyzed its expression in rat liver during 2-AAF/PHx. Three rats per time point were used. The time course from day 1 to day 21 revealed increased miR-133b expression with induction as early as day 5 ( $6.9 \pm 2.3$ ;  $P = 0.07$ ) and up-regulation (4- to 5-fold) reaching

significance at day 7 ( $4.78 \pm 0.52$ ;  $P < 0.01$ ), day 9 ( $4.15 \pm 0.55$ ;  $P < 0.01$ ), day 13 ( $4.54 \pm 0.57$ ;  $P < 0.01$ ), and day 21 ( $4.36 \pm 0.8$ ;  $P < 0.03$ ) compared with normal liver ( $1.18 \pm 0.22$ ) (Figure 2A). Induction at day 9 after 2-AAF/PHx was also observed by reverse transcription ISH

(RT-PCR ISH) using a specific probe for miR-133b (Figure 2B) and positively correlated with Ctgf mRNA up-regulation assessed by Ctgf ISH (Figure 2B).<sup>12</sup> Next, miR-133b was overexpressed in the rat OC line WBF-344 to study effects on Ctgf as a direct molecular target and also effects on proliferation and migration. Semiquantitative PCR revealed that endogenous Ctgf mRNA levels were reduced after 72 hours of miR-133b ectopic expression relative to those of control cells (Figure 2C). To demonstrate that the effects of miR-133b on CTGF mRNA are mediated by the CTGF 3'UTR on rat OCs, we ectopically and transiently expressed CTGF 3'UTR in WBF-344 cells that were transduced with either control or miR-133b—expressing adenovirus (Figure 2D). After 48 hours of transfection with 1  $\mu$ g CTGF 3'UTR containing plasmid, firefly luciferase activity (normalized to renilla) was analyzed by luminometer. A significant decrease in CTGF 3'UTR luciferase activity was observed in WBF-344 cells in the presence of forced miR-133b expression compared with adenovirus control transduced cells ( $1.4 \pm 0.04$  for control versus  $1 \pm 0.08$  for miR-133b;  $P < 0.01$ ) (Figure 2D). In addition, proliferation of miR-133b—overexpressing WBF-344 cells decreased significantly at day 1 ( $42.1\% \pm 6.2\%$ ;  $P < 0.01$ ), 2 ( $27.6\% \pm 3.3\%$ ;  $P < 0.01$ ), and 3 ( $14.3\% \pm 2.5\%$ ;  $P < 0.02$ ) after CTGF stimulation relative to control cells (Figure 2E). Next, we performed a WBF-344 migration assay in the presence or absence of 250 ng/mL recombinant CTGF. Forced expression of miR-133b resulted in a significant reduction ( $30.4\% \pm 7.6\%$ ;  $P < 0.01$ ) of CTGF-induced migration relative to adenovirus control transduced cells (Figure 2F).

#### *In Vivo* miR-133b Adenovirus Delivery Leads to Decreased CTGF Expression and OC Response in the Livers of the 2-AAF/PHx—Treated Rats

To explore the *in vivo* effects of miR-133b overexpression on CTGF expression and OC response during 2-AAF/PHx, GFP only (Ad-control) or GFP-miR-133b (Ad-miR-133b) expressing adenoviruses were delivered intraportally at the time of PHx. Rats were sacrificed at day 7 (data not shown) and day 9. The DR/OC response was present in both groups, as evidenced by the appearance of small cells that were positive for OC markers Sox9 and Ck19 localized around the bile ducts. Also, staining of the liver tissue sections with anti-GFP showed that at day 9 of 2-AAF/PHx, adenovirus transduction of the rat liver cells was present in both GFP control and GFP-miR-133b—expressing groups (Figure 3A). Semiquantitative PCR showed that ectopic miR-133b was expressed *in vivo* in the rat liver (Figure 3B). Both the staining and the quantitation data revealed that there was a reduction of the following: i) Ctgf protein expression ( $3.9 \pm 0.9$  for Ad-control versus  $0.6 \pm 0.2$  for Ad-miR-133b;  $P < 0.01$ ), ii) OC marker Sox9 ( $19.5 \pm 1.6$  versus  $6.2 \pm 1.1$ ;  $P < 0.01$ ), and iii) OC proliferation (Ck19/Ki-67 double-positive cells,  $16.6 \pm 1.4$  versus  $5.6 \pm 0.7$ ;  $P < 0.01$ ), in the livers of the miR-133b—treated group

compared with Ad-control—transduced rats (Figure 3, A and C).

#### Overexpression of miR-133b Inhibits the DR Induced by DDC in Mice

DDC feeding has been widely used to induce progenitor cells and biliary hyperplasia in mouse livers. Recently, we have shown that CTGF plays an important role in regulating DR in this model.<sup>9</sup> To further understand the role of miR-133b in CTGF regulation and DR/OC response, we fed mice with the DDC diet for 1 day to initiate progenitor activation and infected the damaged livers with recombinant adenovirus overexpressing miR-133b through tail vein injection. GFP that was inserted after ribosomal entry sites was coexpressed with miR-133b precursor. In parallel, control viruses that only expressed GFP were administered in mice at equivalent viral titers. Eight days later, animals were sacrificed and DR was analyzed. The immunofluorescence staining detected abundant GFP<sup>+</sup> cells around periportal areas where DDC-induced ductular hyperplasia occurred and intraductal porphyrin pigment plugs were accumulated (Figure 4A). In addition, miR-133b was highly expressed in infected livers in comparison to GFP controls, as shown by TaqMan real-time PCR analysis (Figure 4B). In contrast, CTGF mRNA was significantly down-regulated in livers of all miR-133b virus-infected mice compared with those overexpressing GFP alone at day 8 after DDC feeding (Figure 4C). Immunohistochemistry also detected a lower level of CTGF protein in mice overexpressing miR-133b (Figure 4D). Moreover, reduced biliary proliferation was found in damaged livers infected by miR-133b virus, as revealed by dual immunofluorescence staining for Ki-67 and HPC marker A6 (Figure 4, E and F). Taken together, these observations indicated that ectopic expression of miR-133b inhibited CTGF expression and decreased the DR in murine livers damaged by DDC.

## Discussion

Proper liver function is required to sustain life. Liver can increase functional capacity by adding newly formed hepatocytes to respond to physiological conditions or liver injuries caused by physical trauma or toxicity. Decades of investigation have revealed both the complexity and the importance of well-orchestrated cellular and molecular signals controlling liver regeneration.<sup>38</sup> Moreover, there is an increasing body of evidence about the critical role of miRNAs in liver regeneration and HCC.<sup>18,19</sup> Herein, we explored new control mechanisms important in HCC and OC-mediated liver regeneration. We show the following: i) In HCC patients, miR-133b expression is down-regulated in cancer samples compared with adjacent unaffected liver tissues. ii) Expression of CTGF is decreased in HepG2 cells overexpressing miR-133b. iii) There is reduced CTGF-induced proliferation and migration of HepG2 and WBF-344 cells that overexpress miR-133b. iv)



miR-133b expression is induced in the liver of 2-AAF/PHx-treated rats. v) *In vivo* overexpression of miR-133b via an adenovirus delivery system in the 2-AAF/PHx model of OC activation shows down-regulation of liver CTGF expression, OC marker SOX9, and OC proliferation detected by CK19/Ki-67 costaining. vi) Forced expression of miR-133b decreases endogenous CTGF mRNA and CTGF 3'UTR luciferase activity in WBF-344 rat OCs. and vii) *In vivo* overexpression of miR-133b via adenovirus in the DDC mouse model of OC activation causes down-regulation of CTGF expression and that of proliferating OCs, as measured by A6/Ki-67 costaining.

Song et al<sup>18</sup> have demonstrated that miRNAs are critical regulators of hepatocyte proliferation during liver regeneration (hepatocytes failed to transition to the S phase by 36 hours of two-thirds PHx) by using a mouse model of hepatocyte-specific inactivation of nuclear miRNA processor DGCR8. More important, in this model, authors observed a compensatory expansion of intact OCs. Regarding the contribution of HPCs/DRs/OCs in liver regeneration, there are currently divergent schools of thought in the field.<sup>1,39</sup> Recently, a pericentral Wnt-responsive population of cells that self-renew and contribute to hepatocyte homeostasis has been identified.<sup>40</sup> On the basis of cell fate tracing methods and using the choline-deficient ethionine-supplemented diet model of chronic liver injury, Schaub et al<sup>41</sup> showed that new hepatocytes do not originate from HPCs but from hepatocytes. Furthermore, Tarlow et al<sup>42</sup> presented evidence for a reversible ductular metaplasia of hepatocytes in mice and humans. On the other hand, the clonogenic and the bipotential capacity of HPCs/OCs to differentiate into hepatocytes and biliary cells, and their contribution to liver regeneration, has been demonstrated by several groups, including our laboratory.<sup>2,43</sup> Different outcomes observed in HPC origin and contribution to liver regeneration could be explained by both the heterogeneity of HPC population and differences in animal liver injury models used.<sup>6,38</sup> For example, in contrast to mouse liver injury models, the rat 2-AAF/PHx model of OC activation achieves total inhibition of hepatocyte proliferation, representing a true HPC/DR/OC activation model. Moreover, the mechanisms and signals that control OC activation and proliferation are currently poorly understood. Previously published reports from our laboratory have demonstrated that CTGF is critical to OC activation and that miR-133b directly targets CTGF in rabbit corneal fibroblasts.<sup>12,29</sup> On the other hand, aberrant miRNA expression has been observed in different cancer cell types, and miR-133b has been shown to be down-regulated in several types of cancer, including colorectal and lung cancer.<sup>25</sup> We hypothesized that CTGF regulation by miR-133b is critical to HCC development and OC activation. The decreased miR-133b expression in HCC patient samples and HCC cell lines HepG2 and Huh-7 that we observed is consistent with the general low expression level of miRNAs observed in cancer. Moreover, the reduced cell proliferation and migration combined with decreased CTGF expression seen in HepG2 cells overexpressing miR-133b indicates a tumor suppressor role for

miR-133b that is mediated by CTGF down-regulation. Furthermore, we show that in the rat 2-AAF/PHx model of OC activation, induction of miR-133b is positively correlated with CTGF mRNA expression, representing an example of incoherent miRNA regulatory circuitry.<sup>44,45</sup> This type of regulation avoids background noise and alleviates stochastic fluctuations in gene expression, keeping the target expression level in the optimal range to exercise its effects.<sup>15,46,47</sup> Thus, it is likely that Ctgf expression is tightly controlled by miR-133b during OC activation to avoid premature activation or over-activation of the OC response that could have detrimental consequences for the liver regeneration (ie, fibrosis or cell transformation). In addition, the results of *in vivo* overexpression of miR-133b via adenovirus, which led to reduced Ctgf expression and rat 2-AAF/PHx- or mouse DDC-induced DR/OC response, indicate that miR-133b-induced phenotypic effects are mediated at the molecular level by direct modification of Ctgf expression and that miR-133b overexpression is sufficient to reduce DR/OC response. Although, in this report we present evidence that Ctgf is a direct target modulated by miR-133b in hepatocarcinoma and rat OC lines, and in the rodent liver during OC activation, given the nature of action of miRNAs that regulate multiple targets concomitantly, it is possible that other direct targets of miR-133b involved in liver carcinogenesis and OC response, such as c-MET and CXCR4, also mediate the liver tumor suppression and/or OC response reduction observed herein.<sup>36,48–50</sup>

In conclusion, we present a novel miR-133b/Ctgf regulatory mechanism involved in proliferation and migration of HCC cells and in DR/OC response (Figure 4G). This mechanism could be exploited therapeutically to treat HCC by overexpressing miR-133b either through administration of miR-133b mimics or via virus delivery gene therapy. Moreover, increased miR-133b expression could potentially be used to treat biliary fibrosis given the direct correlation between amplitude of the DRs/OC response and biliary fibrosis. Conversely, miR-133b inhibitors could be used to amplify OC response and enhance liver regeneration.

## Acknowledgments

We thank Dr. William B. Coleman (University of North Carolina at Chapel Hill) and Dr. Chen Liu (University of Florida, Gainesville, FL) for WBF-344 and Huh-7 cells, respectively.

## References

1. Kaur S, Siddiqui H, Bhat MH: Hepatic progenitor cells in action: liver regeneration or fibrosis? *Am J Pathol* 2015, 185:2342–2350
2. Petersen BE, Zajac VF, Michalopoulos GK: Hepatic oval cell activation in response to injury following chemically induced periportal or pericentral damage in rats. *Hepatology* 1998, 27:1030–1038
3. Bisgaard HC, Holmskov U, Santoni-Rugiu E, Nagy P, Nielsen O, Ott P, Hage E, Dalhoff K, Rasmussen LJ, Tygstrup N: Heterogeneity of ductular reactions in adult rat and human liver revealed by novel

- expression of deleted in malignant brain tumor 1. *Am J Pathol* 2002, 161:1187–1198
4. Grisham JW, Coleman WB: Molecular regulation of hepatocyte generation in adult animals. *Am J Pathol* 2002, 161:1107–1110
  5. Gordon GJ, Coleman WB, Grisham JW: Temporal analysis of hepatocyte differentiation by small hepatocyte-like progenitor cells during liver regeneration in retrorsine-exposed rats. *Am J Pathol* 2000, 157:771–786
  6. Petersen BE, Goff JP, Greenberger JS, Michalopoulos GK: Hepatic oval cells express the hematopoietic stem cell marker Thy-1 in the rat. *Hepatology* 1998, 27:433–445
  7. Liedtke C, Luedde T, Sauerbruch T, Scholten D, Streetz K, Tacke F, Tolba R, Trautwein C, Trebicka J, Weiskirchen R: Experimental liver fibrosis research: update on animal models, legal issues and translational aspects. *Fibrogenesis Tissue Repair* 2013, 6:19
  8. Fickert P, Stoger U, Fuchsbichler A, Moustafa T, Marschall HU, Weiglein AH, Tsybrovskyy O, Jaeschke H, Zatloukal K, Denk H, Trauner M: A new xenobiotic-induced mouse model of sclerosing cholangitis and biliary fibrosis. *Am J Pathol* 2007, 171:525–536
  9. Pi L, Robinson PM, Jorgensen M, Oh SH, Brown AR, Weinreb PH, Trinh TL, Yianni P, Liu C, Leask A, Violette SM, Scott EW, Schultz GS, Petersen BE: Connective tissue growth factor and integrin  $\alpha$ 5 $\beta$ 1: a new pair of regulators critical for ductular reaction and biliary fibrosis in mice. *Hepatology* 2015, 61:678–691
  10. Kubota S, Takigawa M: Cellular and molecular actions of CCN2/CTGF and its role under physiological and pathological conditions. *Clin Sci* 2015, 128:181–196
  11. Pi L, Ding X, Jorgensen M, Pan JJ, Oh SH, Pintilie D, Brown A, Song WY, Petersen BE: Connective tissue growth factor with a novel fibronectin binding site promotes cell adhesion and migration during rat oval cell activation. *Hepatology* 2008, 47:996–1004
  12. Pi L, Oh SH, Shupe T, Petersen BE: Role of connective tissue growth factor in oval cell response during liver regeneration after 2-AAF/PHx in rats. *Gastroenterology* 2005, 128:2077–2088
  13. Vidigal JA, Ventura A: The biological functions of miRNAs: lessons from in vivo studies. *Trends Cell Biol* 2015, 25:137–147
  14. van Rooij E: The art of microRNA research. *Circ Res* 2011, 108:219–234
  15. Bartel DP, Chen CZ: Micromanagers of gene expression: the potentially widespread influence of metazoan microRNAs. *Nat Rev Genet* 2004, 5:396–400
  16. Clark AM, Goldstein LD, Tevlin M, Tavare S, Shaham S, Miska EA: The microRNA miR-124 controls gene expression in the sensory nervous system of *Caenorhabditis elegans*. *Nucleic Acids Res* 2010, 38:3780–3793
  17. Choi WY, Giraldez AJ, Schier AF: Target protectors reveal dampening and balancing of Nodal agonist and antagonist by miR-430. *Science* 2007, 318:271–274
  18. Song G, Sharma AD, Roll GR, Ng R, Lee AY, Brelloch RH, Frandsen NM, Willenbring H: MicroRNAs control hepatocyte proliferation during liver regeneration. *Hepatology* 2010, 51:1735–1743
  19. Sun J, Lu H, Wang X, Jin H: MicroRNAs in hepatocellular carcinoma: regulation, function, and clinical implications. *ScientificWorldJournal* 2013, 2013:924206
  20. Mancuso A, Perricone G: Hepatocellular carcinoma and liver transplantation: state of the art. *J Clin Transl Hepatol* 2014, 2:176–181
  21. Gailhouste L, Gomez-Santos L, Hagiwara K, Hatada I, Kitagawa N, Kawaharada K, Thirion M, Kosaka N, Takahashi RU, Shibata T, Miyajima A, Ochiya T: miR-148a plays a pivotal role in the liver by promoting the hepatospecific phenotype and suppressing the invasiveness of transformed cells. *Hepatology* 2013, 58:1153–1165
  22. Hayes J, Peruzzi PP, Lawler S: MicroRNAs in cancer: biomarkers, functions and therapy. *Trends Mol Med* 2014, 20:460–469
  23. Macfarlane LA, Murphy PR: MicroRNA: biogenesis, function and role in cancer. *Curr Genomics* 2010, 11:537–561
  24. Yu H, Lu Y, Li Z, Wang Q: microRNA-133: expression, function and therapeutic potential in muscle diseases and cancer. *Curr Drug Targets* 2014, 15:817–828
  25. Nohata N, Hanazawa T, Enokida H, Seki N: microRNA-1/133a and microRNA-206/133b clusters: dysregulation and functional roles in human cancers. *Oncotarget* 2012, 3:9–21
  26. Duisters RF, Tijssen AJ, Schroen B, Leenders JJ, Lentink V, van der Made I, Herias V, van Leeuwen RE, Schellings MW, Barenbrug P, Maessen JG, Heymans S, Pinto YM, Creemers EE: miR-133 and miR-30 regulate connective tissue growth factor: implications for a role of microRNAs in myocardial matrix remodeling. *Circ Res* 2009, 104:170–178
  27. Roderburg C, Luedde M, Vargas Cardenas D, Vucur M, Mollnow T, Zimmermann HW, Koch A, Hellerbrand C, Weiskirchen R, Frey N, Tacke F, Trautwein C, Luedde T: miR-133a mediates TGF-beta-dependent derepression of collagen synthesis in hepatic stellate cells during liver fibrosis. *J Hepatol* 2013, 58:736–742
  28. Huang J, Yu X, Fries JW, Zhang L, Odenthal M: MicroRNA function in the profibrogenic interplay upon chronic liver disease. *Int J Mol Sci* 2014, 15:9360–9371
  29. Robinson PM, Chuang TD, Sriram S, Pi L, Luo XP, Petersen BE, Schultz GS: MicroRNA signature in wound healing following excimer laser ablation: role of miR-133b on TGFbeta1, CTGF, SMA, and COL1A1 expression levels in rabbit corneal fibroblasts. *Invest Ophthalmol Vis Sci* 2013, 54:6944–6951
  30. Xiu M, Liu YH, Brigstock DR, He FH, Zhang RJ, Gao RP: Connective tissue growth factor is overexpressed in human hepatocellular carcinoma and promotes cell invasion and growth. *World J Gastroenterol* 2012, 18:7070–7078
  31. Wang GB, Zhou XY, Yuan T, Xie J, Guo LP, Gao N, Wang XQ: Significance of serum connective tissue growth factor in patients with hepatocellular carcinoma and relationship with angiogenesis. *World J Surg* 2010, 34:2411–2417
  32. Higgins GM, Anderson RM: Restoration of liver of the white rat following partial surgical removal. *Exp Pathol Liver Arch Pathol* 1931, 12:186–202
  33. Pi L, Jorgensen M, Oh SH, Protopapadakis Y, Gjymishka A, Brown A, Robinson P, Liu C, Scott EW, Schultz GS, Petersen BE: A disintegrin and metalloprotease with thrombospondin type I motif 7: a new protease for connective tissue growth factor in hepatic progenitor/oval cell niche. *Am J Pathol* 2015, 185:1552–1563
  34. Wong TS, Liu XB, Chung-Wai Ho A, Po-Wing Yuen A, Wai-Man Ng R, Ignace Wei W: Identification of pyruvate kinase type M2 as potential oncoprotein in squamous cell carcinoma of tongue through microRNA profiling. *Int J Cancer* 2008, 123:251–257
  35. Kano M, Seki N, Kikkawa N, Fujimura L, Hoshino I, Akutsu Y, Chiyomaru T, Enokida H, Nakagawa M, Matsubara H: miR-145, miR-133a and miR-133b: tumor-suppressive miRNAs target FSCN1 in esophageal squamous cell carcinoma. *Int J Cancer* 2010, 127:2804–2814
  36. Hu G, Chen D, Li X, Yang K, Wang H, Wu W: miR-133b regulates the MET proto-oncogene and inhibits the growth of colorectal cancer cells in vitro and in vivo. *Cancer Biol Ther* 2010, 10:190–197
  37. Mathieu J, Ruohola-Baker H: Regulation of stem cell populations by microRNAs. *Adv Exp Med Biol* 2013, 786:329–351
  38. Shupe TD, Petersen BE: Liver regeneration: a consequence of complex, well-orchestrated signals. *Hepatology* 2015, 62:644–645
  39. Jors S, Jeliakova P, Ringelhan M, Thalhammer J, Durl S, Ferrer J, Sander M, Heikenwalder M, Schmid RM, Siveke JT, Geisler F: Lineage fate of ductular reactions in liver injury and carcinogenesis. *J Clin Invest* 2015, 125:2445–2457
  40. Wang B, Zhao L, Fish M, Logan CY, Nusse R: Self-renewing diploid Axin2(+) cells fuel homeostatic renewal of the liver. *Nature* 2015, 524:180–185

41. Schaub JR, Malato Y, Gormond C, Willenbring H: Evidence against a stem cell origin of new hepatocytes in a common mouse model of chronic liver injury. *Cell Rep* 2014, 8:933–939
42. Tarlow BD, Pelz C, Naugler WE, Wakefield L, Wilson EM, Finegold MJ, Grompe M: Bipotential adult liver progenitors are derived from chronically injured mature hepatocytes. *Cell Stem Cell* 2014, 15:605–618
43. Petersen BE, Zajac VF, Michalopoulos GK: Bile ductular damage induced by methylene dianiline inhibits oval cell activation. *Am J Pathol* 1997, 151:905–909
44. Shkumatava A, Stark A, Sive H, Bartel DP: Coherent but overlapping expression of microRNAs and their targets during vertebrate development. *Genes Dev* 2009, 23:466–481
45. Tsang J, Zhu J, van Oudenaarden A: MicroRNA-mediated feedback and feedforward loops are recurrent network motifs in mammals. *Mol Cell* 2007, 26:753–767
46. Osella M, Bosia C, Cora D, Caselle M: The role of incoherent microRNA-mediated feedforward loops in noise buffering. *PLoS Comput Biol* 2011, 7:e1001101
47. Raser JM, O'Shea EK: Noise in gene expression: origins, consequences, and control. *Science* 2005, 309:2010–2013
48. Duan FT, Qian F, Fang K, Lin KY, Wang WT, Chen YQ: miR-133b, a muscle-specific microRNA, is a novel prognostic marker that participates in the progression of human colorectal cancer via regulation of CXCR4 expression. *Mol Cancer* 2013, 12:164
49. Hatch HM, Zheng D, Jorgensen ML, Petersen BE: SDF-1alpha/CXCR4: a mechanism for hepatic oval cell activation and bone marrow stem cell recruitment to the injured liver of rats. *Cloning Stem Cells* 2002, 4:339–351
50. Li X, Li P, Chang Y, Xu Q, Wu Z, Ma Q, Wang Z: The SDF-1/CXCR4 axis induces epithelial-mesenchymal transition in hepatocellular carcinoma. *Mol Cell Biochem* 2014, 392:77–84